Investigation on the Polarization Dependence of an Angled Polished Multimode Fibre Structure

Ruoning Wang, Ke Tian, Meng Zhang, Yuxuan Jiang, Libo Yuan, Guoyong Jin, Gerald Farrell, *Member*, *OSA*, Elfed Lewis, *Senior Member*, *IEEE* and Pengfei Wang

***Abstract*—An angled polished multimode (APM) fibre structure is described for the first time, to the best our knowledge, and its polarization dependence investigated theoretically and experimentally. Two angled planes are established in the multimode fibre (MMF) section of a single-mode-multimode-single-mode (SMS) fibre structure using the fibre side-polishing technique, forming the APM fibre structure. This designed circular asymmetric geometry induces different propagation characteristics for the TE and TM modes within the MMF. Simulated and experimental results both show that this difference is enhanced as the polishing angle increases, and a maximum extinction ratio (ER) of the spectrum of 13 dB is achieved at a polishing angle of 85°. This polarization-dependent device has a simple fabrication process and is free from the limitation of coating functional materials, which is expected to be applied in non-linear optics, fibre laser and optical fibre sensing fields.**

***Index Terms*—Angled side-polishing, circular asymmetric structure, multimode fibre, polarization dependence.**

I. Introduction

Modulation by polarization plays an important role in photonic devices, fibre lasers and telecommunications systems [1, 2]. To date, various polarizers have been developed to control the state of polarization of light. Among them, a straightforward way to fabricate a polarizer is to use materials with special optical characteristics. Graphene oxide (GO) is a two-dimensional carbon material consisting of hydrophilic oxygen functional groups, and a large attenuation difference between the two orthogonal polarization directions enables it to be a good candidate for applications which utilize polarization modulation [3]. Due to the existence of surface plasmon polarizations (SPPs) supported by metal materials, a variety of metal materials including gold and silver have been used to develop polarizers [4-6]. Crystal materials such as liquid crystals (LCs) are also a good choice to modulate the polarization state, since the LC molecules can be re-orientated by changing the externally applied voltage [7]. These special materials can be relatively easily coated or incorporated on different optical waveguides and fibre structures; however, combining these special materials further increase the complexity and the cost of the designed polarizers.

In addition to using materials with special optical properties, direct fabrication of waveguides with asymmetric geometry structures also provides a new approach for modulations of polarization. To date, asymmetric structures have been successfully introduced in photonic crystal fibres (PCFs) [8], silicon-on-insulator (SOI) systems [9, 10], and a twin waveguide coupling configuration [11]. However, these fabrication methods usually require elaborate design and accurate stacking on the structure, which often leads to complicated manufacturing processes and increased manufacturing cycles.

The fibre side-polishing technique, a simple and effective method for optical fibre processing, has been widely used to fabricate fibre polarizers. In most cases, a flat plane is prepared on the surface of the fibre to form a well-known D-shaped fibre, and this flat surface is often used to provide a substrate for different coating materials [12]. For instance, birefringent crystals [13, 14], a polymer overlay [15], a single layer of thin aluminum [16] and single or double graphene stacks [17, 18] have been adopted and coated on the flat surface of a D-shaped fibre, and the realized ERs for the fabricated side polished polarizers were as high as 60, 60, 36, 22.6, 27 and 36 dB,

This work was supported in part by the Key Program of the National Natural Science Foundation of China (NSFC) under Grant 61935006; in part by the Key Program for Natural Science Foundation of Heilongjiang Province of China under Grant ZD2016012; in part by the Fundamental Research Funds for the Central Universities under Grant 3072020CFJ2507; and in part by the 111 project (B13015) to the Harbin Engineering University. Professor Elfed Lewis is co-author on this publication and is supported by Science Foundation Ireland under the Centre research program (SFI/12/RC/2302_P2) for the MaREI project. (*Corresponding author: Ke Tian and Pengfei Wang*)

R. Wang, K. Tian, M. Zhang, Y. Jiang and P. Wang are with the Key Laboratory of In-fiber Integrated Optics of Ministry of Education, College of Science, Harbin Engineering University, Harbin 150001, China (e-mail: ruonwang@hrbeu.edu.cn; ketian@hrbeu.edu.cn; mengzhang@hrbeu.edu.cn; merak@hrbeu.edu.cn; pengfei.wang@tudublin.ie).

L. Yuan is with the Photonics Research Center, Guilin University of Electronic Technology, Guilin, China (e-mail: lbyuan@vip.sina.com).

K. Tian and G. Jin are with the College of Power and Energy Engineering, Harbin Engineering University, Harbin 150001, China (e-mail: ketian@hrbeu.edu.cn; guoyongjin@hrbeu.edu.cn).

G. Farrell is with the Photonics Research Centre, Technological University Dublin, Ireland (e-mail: gerald.farrell@dit.ie).

E. Lewis is with the Optical Fibre Sensors Research Centre, Department of Electronic and Computer Engineering, University of Limerick, Limerick, Ireland (e-mail: Elfed.Lewis@ul.ie).

P. Wang is also with the Key Laboratory of Optoelectronic Devices and Systems of Ministry of Education and Guangdong Province, College of Optoelectronic Engineering, Shenzhen University, Shenzhen 518060, China. (e-mail: pengfei.wang@tudublin.ie).

respectively. Although these polarizers prepared using the fiber side-polishing technology combined with the functional materials coating offer good polarization performance, the high cost and low stability caused by the need for external coating materials are unavoidable.

In this article, an angled polished multimode (APM) fibre structure is described and its polarization dependence investigated theoretically and experimentally. It differs most significantly from normal polarizers which rely on the use of functional coating materials, whereas this APM fibre structure consists only of two planes with a specific polishing angle. The achieved circular asymmetric geometry results in different propagation characteristics for the TE and TM modes within the fibre. Both simulated and experimental results demonstrate that the polarization ER is improved as the polishing angle increases. The APM fibre samples with different fabrication parameters have been prepared experimentally, and a maximum ER of the spectrum of 13 dB is achieved with a polishing angle of 85°. Such a polarization-dependent device is free from the limitation imposed by the need for a functional coating material, which makes it a promising polarizer for use in the photonics field.

II. Theoretical Analysis and Device Fabrication

The schematic diagram of the APM fibre structure is illustrated in Fig. 1. The APM fibre structure consists of an SMS fibre structure where the MMF section was side polished in two different locations to form polished planes, each with a specific polishing angle. It can be seen from Fig. 1 that the two polished planes are angled to each other but that the polishing depth (PD) of the two polishing planes are the same. In this case, the acute angle between two polished planes is defined as θ.

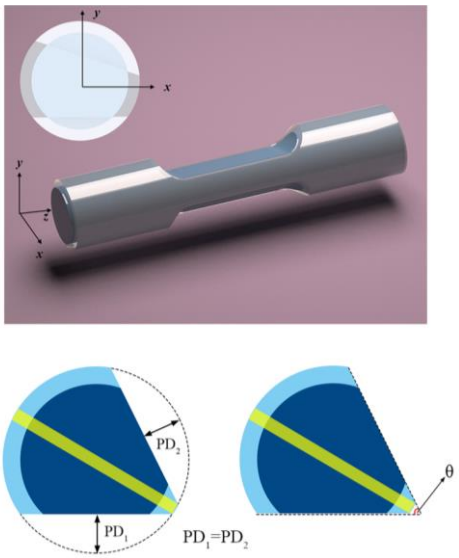

Fig. 1. Schematic diagram of the cross section of the angled polished MMF.

In order to determine the light propagation inside the fibre structure, a one-way guided-mode propagation theory is used to analyze the excited modes within MMF [19]. Given the circular symmetry of the fundamental mode (LP_{01}) within SMF core, the input Gaussian beam is assumed to have a spatial field distribution of $E(x, y, 0)$ [20]. In this case both the offset of the alignment between SMF and MMF and the radiation from MMF are neglected, hence only the LP_{0m} modes of the MMF can be excited when the light launches into the MMF. The exited modes number of LP_{0m} can be calculated using

$$M = \frac{V}{\pi} = \frac{2r}{\lambda}\sqrt{n_{co}^2 - n_{cl}^2} \tag{1}$$

where r is the radius of MMF, n_{co} and n_{cl} are the refractive index (RI) for the core and cladding of the MMF, respectively, and λ is the wavelength in the free-space.

Denoting the field distribution of the LP_{0m} modes as $F_m(x, y)$, the input light field distribution can be expressed as [21]

$$E(x, y, 0) = \sum_{m=1}^{M} c_m F_m(x, y) \tag{2}$$

where c_m is the exciting coefficient of m-th order mode which is defined as [22]

$$c_m = \frac{\int_0^\infty \int_0^\infty E(x,y,0) F_m(x,y) dxdy}{\int_0^\infty \int_0^\infty F_m(x,y) F_m(x,y) dxdy} \tag{3}$$

Therefore, the light field inside MMF at the propagation length of z can be expressed as [23, 24]

$$E(x,y,z) = \sum_{m=1}^{M} c_m F_m(x,y) exp(i\beta_m z) \tag{4}$$

where β_m is the propagation constant of the m-th order mode of MMF.

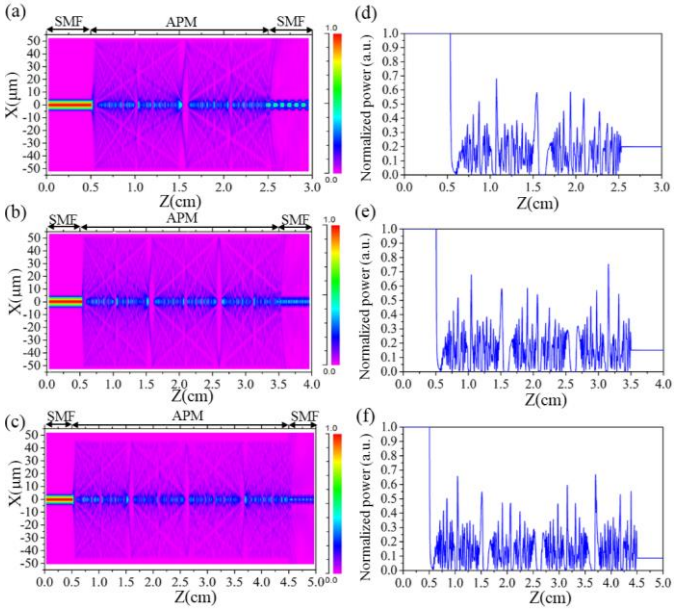

Fig. 2. Simulated optical field distribution within an APM fibre structure with different propagation length (a) 2 cm; (b) 3 cm; (c) 4 cm. (d)-(f) are the intensity distribution of the output optical field corresponding to the cases in (a)-(c).

Numerical simulations have been carried out using a full vector Beam Propagation Method (BPM) to further investigate the light field distribution within an APM fibre structure. The input optical field is Gaussian and is launched using a length of SMF. The mesh size in the profile direction (x, y) and propagation direction (z) were set to be 0.1 μm, 0.1 μm, and 10 μm, respectively. The core/cladding diameter and RI of the SMF and MMF used in the simulation were 8.3/125 μm and 1.4504/1.4447, 105/125 μm and 1.4446/1.4271, respectively.

The polishing angle θ and PD were set to be 70° and 20 μm, respectively. MMFs with lengths of 2 cm, 3 cm and 4 cm were chosen for the simulation since these lengths are neither too long nor too short for practical cutting and polishing and are typical of the MMF lengths found in previously reported SMS structures [25].

When the input wavelength was set to 1550 nm, the simulated optical field distribution results are shown in Fig. 2. It can be seen from Fig. 2(a)-(c) that there is no clear difference between the propagation patterns of the propagation optical field as the MMF length is increased from 2 to 4 cm. It means that the length of MMF does not have a direct effect on the propagation characteristics of the APM fibre structure. However, it can be seen from the simulated results in Fig. 3 that the SMS fibre structure with a length of 4 cm MMF has better spectral visibility, which is also consistent with results reported in previous articles [23, 26]. In addition, an SMS fibre structure composed of a shorter MMF is difficult to observe (locate) and is more easily broken during the polishing process. Therefore, an MMF with a length of 4 cm was adopted to fabricate the APM fibre structure in this investigation.

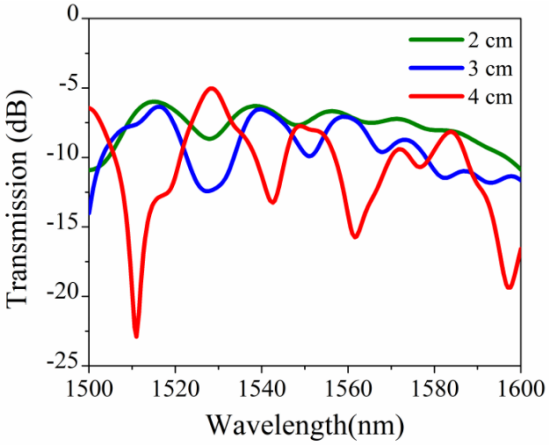

Fig. 3. The simulated spectra of SMS fibre structure with the MMF length of 2 cm, 3 cm and 4 cm.

The polarization dependence of the APM fibre structure of this investigation depends on the noncircular geometry formed by side-polishing. As shown in Fig. 1, the yellow-marked region is the portion of the MMF which still retains a circular symmetry and the other portion has a noncircular symmetry following angled polishing. The unmarked parts can be considered as corresponding to having an elliptical core and these elliptical core-like parts cause the differences in propagation between the TE and TM modes. It is worth noting that the noncircular geometry must penetrate into the fibre core, as penetration into the fibre cladding alone would have no effect on the TE and TM modes [27]. For example, the cladding of a D-shaped fibre is polished, but its core is still circularly symmetrical, which presents no polarization dependence [18]. In this investigation, a MMF was chosen because it has a larger core size, so it does not require an excessive polishing depth compared to an SMF. However, it is necessary to determine an effective PD for the MMF which induces differences in the propagation of the TE and TM modes.

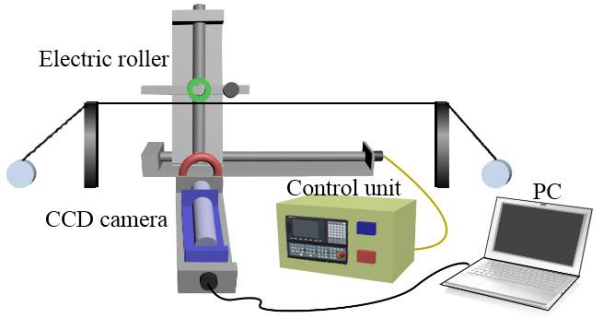

Fig. 4. Schematic diagram of the experimental setup for angled polishing MMF.

The influence of the PD on the output optical field distribution of the APM fibre structure was explored as well as determining an effective PD. For this purpose, APM fibre samples with different PD values but the same MMF length of 4 cm and a polishing angle of 70° were fabricated using an accurate fibre polishing system. The fibre polishing system is shown in Fig. 4, which consists of three main parts, namely an electric roller, a CCD observation system and a control unit. The outside surface of the electric roller was covered with a layer of abrasive paper for polishing the MMF. The choice of roughness of the used abrasive paper was dictated as a result of a trade-off between polishing smoothness and polishing time. Based on previous work [28], the abrasive paper with 800 mesh roughness was selected to polish the MMF. The electric roller can move back and forth horizontally while rotating to produce different polishing lengths. The rotation speed and horizontal movement speed of the roller was tuned using an automatic control unit. The CCD camera was connected to a PC for real-time monitoring of the PD of the MMF.

Before polishing the MMF, a traditional SMS fibre structure was prepared by coupling a 4 cm length MMF (AFS105/125Y) between two sections of single-mode fibres (SMF-28). The fabrication process of the APM fibre structure is relatively simple and can be divided into three steps. Firstly, the SMS fibre sample was fixed with two fibre clampers, ensuring that the pre-polished section was positioned at the midpoint of the two fibre clampers. The second step was to set specific polishing parameters including the polishing length and PD in the control unit. When a single-side polished MMF was obtained, the SMS fibre sample was accurately rotated to the required angle. Finally, the above step 2 was repeated to fabricate the second polished side and complete the APM fibre structure.

The microscope images of the cross section of the fabricated APM fibre samples are shown in Fig. 5(a)-(d), which have different PDs of 0 μm, 10 μm, 15 μm and 20 μm, respectively. In order to investigate the influence of the PD on the output optical field distribution of the APM fibre structure, the optical field distribution profile was measured using a laser beam profiler (Newport, LBP2), and the corresponding three-dimensional (3D) results are shown in Fig. 5(e)-(h). It can be seen that when the MMF is unpolished, the optical field intensity along the x axial and y axial directions is symmetric as expected. When the angled polished MMFs have PDs of 10 μm and 15 μm, the profile optical field distribution is still

approximately symmetrical. However, as the PD was increased to 20 μm, the output optical field intensity along the x axial and y axial directions changes dramatically. These initial exploratory experiments demonstrated that a polishing depth of 20 μm is a feasible value for investigating polarization dependence of the APM fibre structure.

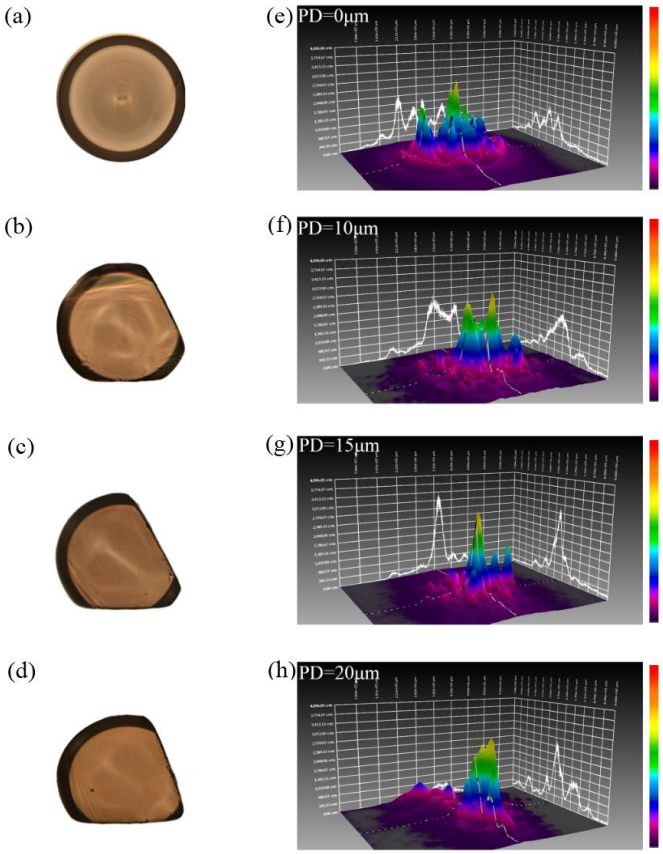

Fig. 5. Microscopic images of the cross section of the APM fibre samples with different PD (a) PD=0 μm; (b) PD=10 μm; (c) PD=15 μm; (d) PD=20 μm. (e)-(h) are the 3D images of the output optical field distribution corresponding to the cases in (a)-(d).

Based on the above exploration of fabrication parameters, three samples with selected MMF length of 4 cm and PD of 20 μm but with different polishing angles of 45˚, 65˚ and 85˚ were prepared, which are identified as Sample 1, Sample 2 and Sample 3, respectively in this article. The corresponding cross section microscopic images of the three samples are shown in Fig. 6(a)-(c).

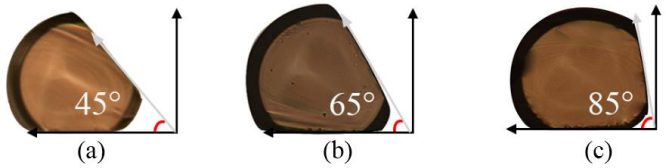

Fig. 6. Microscopic images of the cross section of the angled polished MMF samples with different polishing angles (a) θ=45° (sample 1); (b) θ=65° (sample 2); (c) θ=85° (sample 3).

III. Experiments and Discussion

Fig. 7 illustrates the experimental setup for spectral polarization dependence measurement. The free ends of the APM fibre structure were fixed using two fibre clampers to prevent bending of the structure. A supercontinuum source (YSL, SC Series) was used to provide the input light signal, and the output light signal was recorded using a high resolution (0.02 nm) optical spectrum analyzer (OSA, YOKOGAWA AQ6370D). A polarization controller was linked within the light path to change the state of polarization of the input light, and the resulting polarization angle is defined as β.

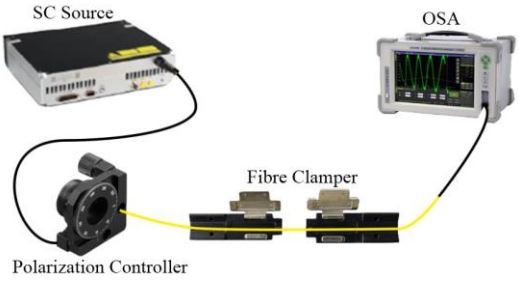

Fig. 7. Experimental setup for the extinction ratio measurement.

Numerical simulations were carried out to predict the spectral polarization dependence of the APM fibre structure. As shown in Fig. 8(a)-(c), the spectra in the TE mode have a smaller transmission loss compared to the cases in the TM mode. The largest ERs of Sample 1, 2, 3 were calculated to be 3 dB, 5 dB and 6.5 dB, respectively. The simulated results show that the APM fibre structure exhibits a distinct polarization dependence, and this dependence is enhanced with an increase in the polishing angle.

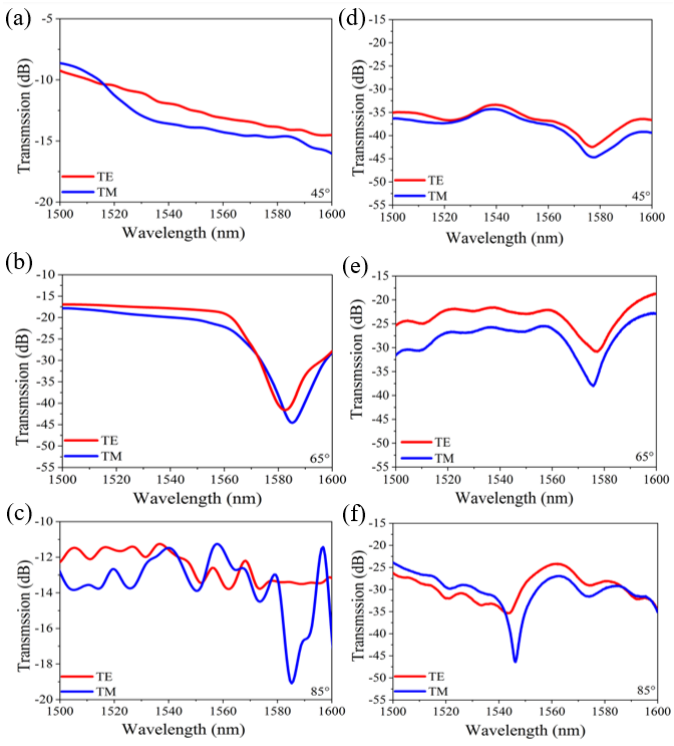

Fig. 8. Simulated spectral polarization dependence of (a) Sample 1; (b) Sample 2; (c) Sample 3. Measured spectral polarization dependence of (d) Sample 1; (e) Sample 2; (f) Sample 3.

Fig. 8(d)-(f) are the corresponding experimental spectral responses of Sample 1, 2, and 3 in different states of polarization. It can be seen that the measured results are in general agreement with the simulated results, in which the transmission loss of spectra in the TM mode is higher than in the TE mode. Moreover, the measured results also confirmed the polarization dependence of the APM structure on the polishing angle. The largest ERs of Sample 1, 2, 3 were 2.5 dB, 7.5 dB and 13 dB, achieved at wavelength of 1577, 1575, 1546 nm, respectively. The effective bandwidth of the samples is about 10 nm in each case. The discrepancies between the measured and simulated results can be explained as the inevitable polish surface roughness is difficult to include in the simulation model. Both the simulated and measured results show that the APM fibre structure has a greater effect on the propagation within TE and TM mode as θ increases, and hence results in a greater separation of the light intensity distribution in these modes.

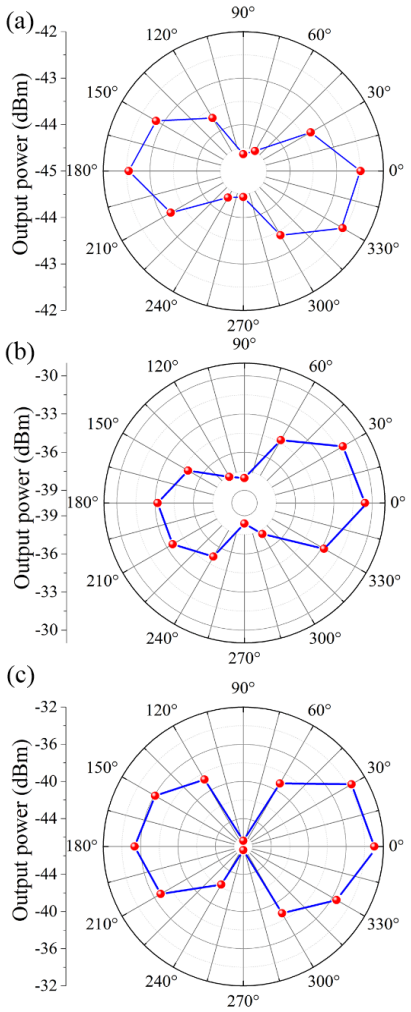

Fig. 9. Polar images of the output power (a) Sample 1 at the wavelength of 1577 nm; (b) Sample 2 at the wavelength of 1575 nm; (c) Sample 3 at the wavelength of 1546 nm.

The output power of three samples at the dip wavelengths of 1577 nm, 1575, and 1546 nm in different polarization states were also monitored using a power meter. The input light was provided by a continuous wave (CW) tunable laser (TSL-510) with an output power of -15 dBm. The total insertion loss of the three samples was found to be in the range 8.5-9.5 dB which is introduced by the angled polishing process. This insertion loss value is similar to those the previously reported literature [17, 18]. However, this value is still large for many practical applications. β was changed from 0° to 360° with a step of 30°, and the corresponding polar plot at the wavelength of 1577, 1575, and 1546 nm for Sample 1, 2, and 3 are shown in Fig. 8. It can be seen from Fig. 9(a)-(c) that the largest output power occurs in the TE mode for which β was 0°or 180°, and the smallest values occurs in the TM mode for which β was 90° or 270°. This characteristic was observed in all samples, which confirms that the APM fibre structure exhibits a controllable polarization dependence. The angled polishing method disrupts the standard circular symmetry of the MMF and brings differences in the propagation of different polarization modes, and such a difference can be tuned using θ.

IV. Conclusion

In this article, to the best of our knowledge, an APM fibre structure has been investigated for the first time and its polarization dependence determined theoretically and experimentally. Using the fibre side-polishing technique, the circular symmetry of the MMF was destroyed, which results the difference in the propagation of the TE and TM modes. Both the simulated and experimental results show that the spectral polarization dependence was enhanced as the polishing angle increases. Three samples with the same PD but different polishing angles were prepared and a maximum ER for the spectrum of 13 dB was achieved at a polishing angle of 85°. This polarization-dependent device has a simple fabrication process and does not require functional material coating, and is therefore expected to be applied in the non-linear optics, fibre laser and optical fibre sensing fields.

References

[1] J. Fatome, S. Pitois, P. Morin, and G. Millot, "Observation of light-by-light polarization control and stabilization in optical fibre for telecommunication applications," *Optics Express*, vol. 18, no. 15, pp. 15311-15317, 2010.

[2] D. Dai, J. Bauters, and J. E. Bowers, "Passive technologies for future large-scale photonic integrated circuits on silicon: polarization handling, light non-reciprocity and loss reduction," *Light: Science & Applications*, vol. 1, no. 3, pp. e1-e1, 2012.

[3] H. Ahmad, M. T. Rahman, M. J. Faruki, S. R. Azzuhri, M. F. Ismail, N. M. S. Shah, and M. Z. A. Razak, "Graphene oxide (GO)-based wideband optical polarizer using a non-adiabatic microfiber," *Journal of Modern Optics*, vol. 64, no. 5, pp. 439-444, 2017.

[4] W. L. Barnes, A. Dereux, and T. W. Ebbesen, "Surface plasmon subwavelength optics," *Nature*, vol. 424, no. 6950, pp. 824-830, 2003.

[5] Y. Ma, G. Farrell, Y. Semenova, B. Li, J. Yuan, X. Sang, B. Yan, C. Yu, T. Guo, and Q. Wu, "Optical microfiber-loaded surface plasmonic TE-pass polarizer," *Optics & Laser Technology*, vol. 78, pp. 101-105, 2016.

[6] A. M. Mahros, M. M. Tharwat, and I. Ashry, "Investigating the characteristics of TM-pass/TE-stop polarizer designed using plasmonic nanostructures," *Applied Optics*, vol. 54, no. 14, pp. 4464-4470, 2015.

[7] D. C. Zografopoulos, G. Isić, E. E. Kriezis, and R. Beccherelli, "A switchable circular polarizer based on zenithal bistable liquid crystal gratings," *Journal of Physics D: Applied Physics*, vol. 49, no. 19, p. 195104, 2016.

[8] B. Sun, M.-y. Chen, R.-j. Yu, Y.-k. Zhang, and J. Zhou, "Design of a fiber polarizer based on an asymmetric dual-core photonic crystal fiber," *Optoelectronics Letters*, vol. 7, no. 4, p. 253, 2011.
[9] H. Xu and Y. Shi, "On-Chip Silicon TE-Pass Polarizer Based on Asymmetrical Directional Couplers," *IEEE Photonics Technology Letters*, vol. 29, no. 11, pp. 861-864, 2017.
[10] X. Sun, M. Mojahedi, and J. S. Aitchison, "Hybrid plasmonic waveguide-based ultra-low insertion loss transverse electric-pass polarizer," *Optics Letters*, vol. 41, no. 17, pp. 4020-4023, 2016.
[11] A. Wieczorek, B. Roycroft, J. O. Callaghan, K. Thomas, E. Pelucchi, F. H. Peters, and B. Corbett, "Polarizers in an Asymmetric Twin Waveguide Based on Resonant Coupling," *IEEE Photonics Technology Letters*, vol. 25, no. 14, pp. 1301-1304, 2013.
[12] X. Wang, G. Farrell, E. Lewis, K. Tian, L. Yuan, and P. Wang, "A Humidity Sensor Based on a Singlemode-Side Polished Multimode–Singlemode Optical Fibre Structure Coated with Gelatin," *Journal of Lightwave Technology*, vol. 35, no. 18, pp. 4087-4094, 2017.
[13] R. A. Bergh, H. C. Lefevre, and H. J. Shaw, "Single-mode fiber-optic polarizer," *Optics Letters*, vol. 5, no. 11, pp. 479-481, 1980.
[14] M. Ssu-Pin and T. Shiao-Min, "High-performance side-polished fibers and applications as liquid crystal clad fiber polarizers," *Journal of Lightwave Technology*, vol. 15, no. 8, pp. 1554-1558, 1997.
[15] S. G. Lee, J. P. Sokoloff, B. P. McGinnis, and H. Sasabe, "Fabrication of a side-polished fiber polarizer with a birefringent polymer overlay," *Optics Letters*, vol. 22, no. 9, pp. 606-608, 1997.
[16] X. Wang, W. Chaojun, and Z. Wang, "In-line fiber-optical polarizer with high-extinction ratios and low-insertion loss," *Microwave and Optical Technology Letters*, vol. 51, no. 7, pp. 1763-1765, 2009.
[17] Q. Bao, H. Zhang, B. Wang, Z. Ni, C. H. Y. X. Lim, Y. Wang, D. Y. Tang, and K. P. Loh, "Broadband graphene polarizer," *Nature Photonics*, vol. 5, no. 7, pp. 411-415, 2011.
[18] R. Chu, C. Guan, J. Yang, Z. Zhu, P. Li, J. Shi, P. Tian, L. Yuan, and G. Brambilla, "High extinction ratio D-shaped fiber polarizers coated by a double graphene/PMMA stack," *Optics Express*, vol. 25, no. 12, pp. 13278-13285, 2017.
[19] Q. Wang, G. Farrell, and W. Yan, "Investigation on Single-Mode–Multimode– Single-Mode Fiber Structure," *Journal of Lightwave Technology*, vol. 26, no. 5, pp. 512-519, 2008.
[20] W. S. Mohammed, A. Mehta, and E. G. Johnson, "Wavelength Tunable Fiber Lens Based on Multimode Interference," *Journal of Lightwave Technology*, vol. 22, no. 2, p. 469, 2004.
[21] K. Tian, G. Farrell, X. Wang, W. Yang, Y. Xin, H. Liang, E. Lewis, and P. Wang, "Strain sensor based on gourd-shaped single-mode-multimode-single-mode hybrid optical fibre structure," *Optics Express*, vol. 25, no. 16, pp. 18885-18896, 2017.
[22] H. Dong, L. Chen, J. Zhou, J. Yu, H. Guan, W. Qiu, J. Dong, H. Lu, J. Tang, W. Zhu, Z. Cai, Y. Xiao, J. Zhang, and Z. Chen, "Coreless side-polished fiber: a novel fiber structure for multimode interference and highly sensitive refractive index sensors," *Optics Express*, vol. 25, no. 5, pp. 5352-5365, 2017.
[23] J. Tang, J. Zhou, J. Guan, S. Long, J. Yu, H. Guan, H. Lu, Y. Luo, J. Zhang, and Z. Chen, "Fabrication of Side-Polished Single Mode-Multimode-Single Mode Fiber and Its Characteristics of Refractive Index Sensing," *IEEE Journal of Selected Topics in Quantum Electronics*, vol. 23, no. 2, pp. 238-245, 2017.
[24] X. Wang, J. Zhang, K. Tian, S. Wang, L. Yuan, E. Lewis, G. Farrell, and P. Wang, "Investigation of a novel SMS fiber based planar multimode waveguide and its sensing performance," *Optics Express*, vol. 26, no. 20, pp. 26534-26543, 2018.
[25] Y. Cardona-Maya, I. D. Villar, A. B. Socorro, J. M. Corres, I. R. Matias, and J. F. Botero-Cadavid, "Wavelength and Phase Detection Based SMS Fiber Sensors Optimized With Etching and Nanodeposition," *Journal of Lightwave Technology*, vol. 35, no. 17, pp. 3743-3749, 2017.
[26] K. Tian, G. Farrell, X. Wang, Y. Xin, Y. Du, W. Yang, H. Liang, E. Lewis, and P. Wang, "High sensitivity temperature sensor based on singlemode-no-core-singlemode fibre structure and alcohol," *Sensors and Actuators A: Physical*, vol. 284, pp. 28-34, 2018.
[27] G. L. Yip and H. H. Yao, "Numerical study of radially inhomogeneous optical fibers using a predictor–corrector method," *Applied Optics*, vol. 21, no. 23, pp. 4308-4315, 1982.
[28] X. Wang, K. Tian, L. Yuan, E. Lewis, G. Farrell, and P. Wang, "A High-Temperature Humidity Sensor Based on a Singlemode-Side Polished Multimode-Singlemode Fiber Structure," *Journal of Lightwave Technology*, vol. 36, no. 13, pp. 2730-2736, 2018.